



LAWRENCE
LIVERMORE
NATIONAL
LABORATORY

Review of High-Speed Fiber Optic Grating Sensors Systems

E. Udd, J. Benterou, C. May, S. J. Mihailov, P. Lu

March 29, 2010

SPIE Defense, Security and Sensing, 7677-Fiber Optic
Sensors and Applications VII
Orlando, FL, United States
April 5, 2010 through April 9, 2010

Disclaimer

This document was prepared as an account of work sponsored by an agency of the United States government. Neither the United States government nor Lawrence Livermore National Security, LLC, nor any of their employees makes any warranty, expressed or implied, or assumes any legal liability or responsibility for the accuracy, completeness, or usefulness of any information, apparatus, product, or process disclosed, or represents that its use would not infringe privately owned rights. Reference herein to any specific commercial product, process, or service by trade name, trademark, manufacturer, or otherwise does not necessarily constitute or imply its endorsement, recommendation, or favoring by the United States government or Lawrence Livermore National Security, LLC. The views and opinions of authors expressed herein do not necessarily state or reflect those of the United States government or Lawrence Livermore National Security, LLC, and shall not be used for advertising or product endorsement purposes.

Review of High-Speed Fiber Optic Grating Sensor Systems

Eric Udd

Columbia Gorge Research, LLC, 2555 NE 205th Avenue, Fairview, Oregon 97024

Jerry Benterou and Chadd May

Lawrence Livermore National Laboratory, 7000 East Avenue, Livermore, California 94550

Stephen J. Mihailov and Ping Lu

Communication Research Centre-Canada, 3701 Carling Avenue, Ottawa K2H8S2

ABSTRACT

Fiber grating sensors can be used to support a wide variety of high speed measurement applications. This includes measurements of vibrations on bridges, traffic monitoring on freeways, ultrasonic detection to support non-destructive tests on metal plates and providing details of detonation events. This paper provides a brief overview of some of the techniques that have been used to support high speed measurements using fiber grating sensors over frequency ranges from 10s of kHz, to MHz and finally toward frequencies approaching the GHz regime.

Keywords: Fiber gratings, high speed, velocity sensor, detonation, Bragg grating

1. Introduction

Very early in the development of fiber grating sensor systems it was realized that a high speed fiber grating sensor system could be realized by placing an optical filter that might be a fiber grating in front of a detector so that spectral changes in the reflection from a fiber grating were amplitude modulated [1-3]. In principal the only limitation on this type of system involved the speed of the output detector which with the development of high speed communication links moved from the regime of 10s of MHz toward 10s of GHz. The earliest deployed systems involved civil structures including measurements of the strain fields on composite utility poles and missile bodies during break tests [4-8], bridges and freeways [9-15, 17-19, 21, 23]. This was followed by a series of developments that included high speed fiber grating sensors to support nondestructive testing via ultrasonic wave detection [16], high speed machining [20] and monitoring ship hulls [22]. Each of these applications involved monitoring mechanical motion of structures and thus interest was in speeds up to a few 10s of MHz. Most recently there has been interest in using fiber grating to monitor the very high speed events such as detonations [24-26] and this has led to utilization of fiber gratings that are consumed during an event that may require detection speeds of hundreds of MHz and in the future multiple GHz.

2. Fiber-optic Bragg grating sensors: For Structural Monitoring

Some of the earliest work involving high speed fiber grating sensor system utilized a fiber grating filter positioned so that the filter slope was at or near the center of the spectral profile associated with the high speed fiber grating sensor. This type of dynamic system is shown in block diagram form by Figure 1 where the sensor may be embedded in a roadway or bridge. In this case a broad band light source that might be a light emitting diode or fiber light source is coupled to a beamsplitter and used to illuminate a fiber grating embedded or attached to a structure. The light spectrum from the sensor is then reflected back through the beamsplitter and directed onto a second beamsplitter. The second beamsplitter then directs one light beam

to a reference detector without an optical filter and a second light beam through an optical filter onto a second detector. The optical filter that can be a second fiber grating whose spectrum is offset from the sensor grating is used to convert spectral changes from the sensor grating to an amplitude modulated output. By taking the ratio of the output of the reference detector to the spectral filtered signal on the second detector extraneous amplitude induced errors can be minimized. Fundamentally the speed of this type of system is limited solely by the speed of the output detectors that can be on the order of GHz.

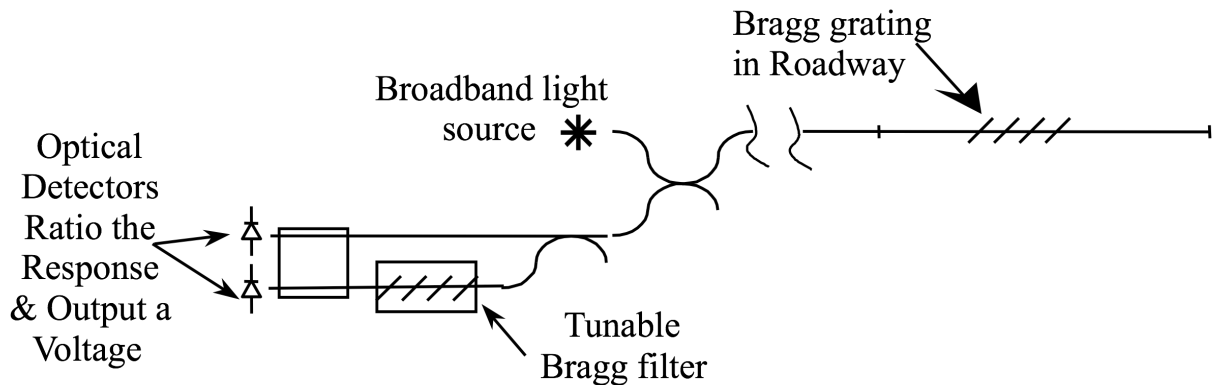


Figure 1. High speed fiber grating sensor systems may be configured using a spectrally broadband light source to illuminate the sensing fiber in combination with a spectrally sloped optical filter placed in front of a high speed detector.

Examples of the utilization of this type of system include the deployment of 0.7 and 1.0 m fiber grating based sensors placed in the Horsetail Falls Bridge in the Columbia River Gorge of Oregon in 1998. These sensors consisted of lengths of prestrained optical fiber in tubes that were anchored on each end and attached to composite reinforce beams on this historic bridge. Twenty seven sensors were attached and one placed in tension on the bottom of a central beam was used in an early demonstration of traffic monitoring in 1999 illustrated by Figure 2.

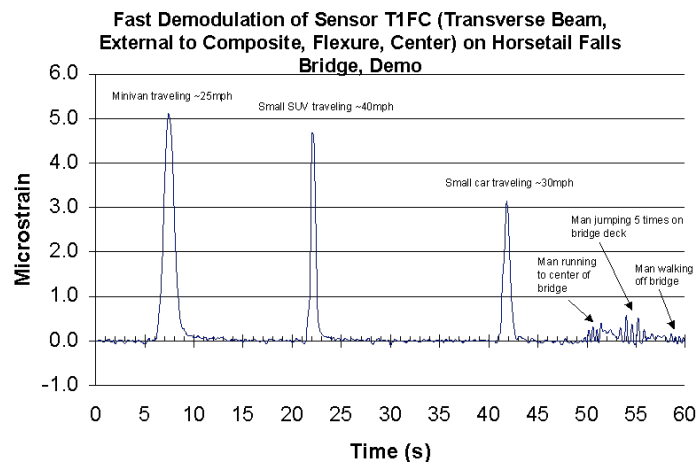


Figure 2. High speed fiber gratings using the system illustrated by Figure 1 were used to measure the speed and weight of a minivan, small SUV, a small car and a jogger in 1999.

In the 1999 demonstration it was possible to monitor the weight of vehicles by looking at the full width half maximum of the signal and to measure the weight by the strain level on the bridge beam. During this test a 70 kg jogger came along and ran, jumped and walked off the bridge all with clearly discernable signals.

A second application involved placing fiber grating sensors at a depth of approximately 8 cm into the concrete bed of the I-84 freeway near exit 14 in 2000. The installation of the first set of four one m long prestrained sensors at this location is shown in Figure 3.



Figure 3. Installation of a set of four prestrained fiber grating sensors into the I 84 freeway near exit 14 in 2000.

The principal objection of the fiber grating sensors located in the I 84 freeway was to identify the types of trailers being towed by axle spacing.

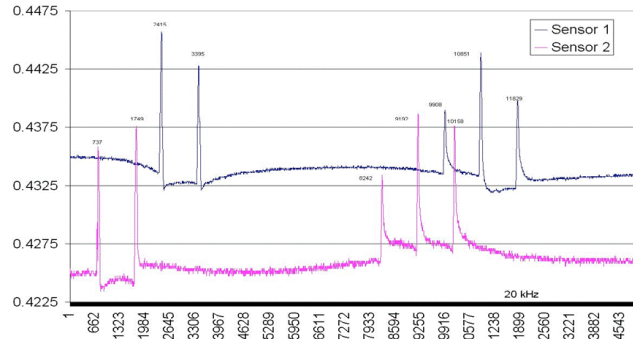


Figure 4. A trailer truck and its signature from two high speed fiber grating sensor located on I 84 near exit 14.

Figure 4 shows the signal from two of the fiber gratings that are spaced on the freeway. It clearly shows each of the five axles of the truck and their spacing. The signatures have sufficient resolution that the speed of the vehicle can also be measured with less than one per cent error. The system had sufficient sensitivity that it could detect the speed and position of the small car passing in the traffic lane adjacent to the lane containing the fiber sensors.

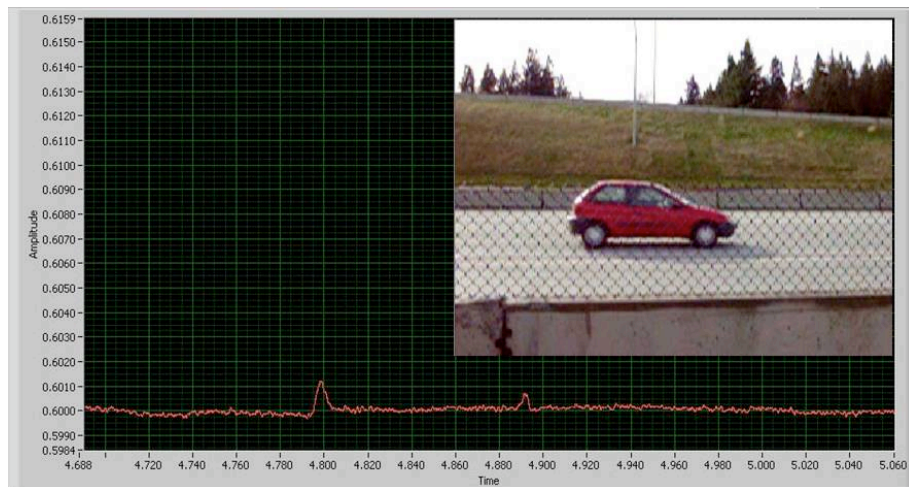


Figure 5. Signature from a small car passing in a lane adjacent to the fiber grating sensors embedded in the I 84 freeway near exit 14.

Higher sensitivity than that associated with the system of Figure 1 can be obtained by using a system based on a higher power tunable light source directed at the center of the spectral slope of a fiber grating. An early implementation of this involved using an ASE light source with an etalon placed in front of it to form a narrow band tunable light source that was used measure vibrations on bridge steel beams. By detecting the modes of vibration of the beams the damage state of the bridge could be assessed.

3. Fiber-optic Bragg grating sensors: For Detonation Monitoring

Chirped fiber-optic Bragg gratings (CFBGs) have been used in the telecom industry for over a decade and are now readily available on the commercial market. Standard and customized CFBGs can be purchased from manufacturers with various physical lengths and optical characteristics. CFBGs reflect a narrow band of the optical spectrum while allowing light outside that band to pass through (figure 6). Grating manufacturers can customize the bandwidth, chirp rate, physical length and reflectivity of these gratings. In

the case of using embedded CFBGs for detonation monitoring, a grating is chosen where the reflection bandwidth and physical length are known. By knowing the relationship between reflection bandwidth and physical length, it is possible to indirectly monitor the length of the embedded grating during a fast moving detonation, thus giving a length vs. time history during a detonation. The CFBGs that were used in the detonation experiments described in this paper were manufactured at the Communications Research Centre-Canada (CRC). The researchers at CRC were very accommodating and were able to create gratings according to specifications.

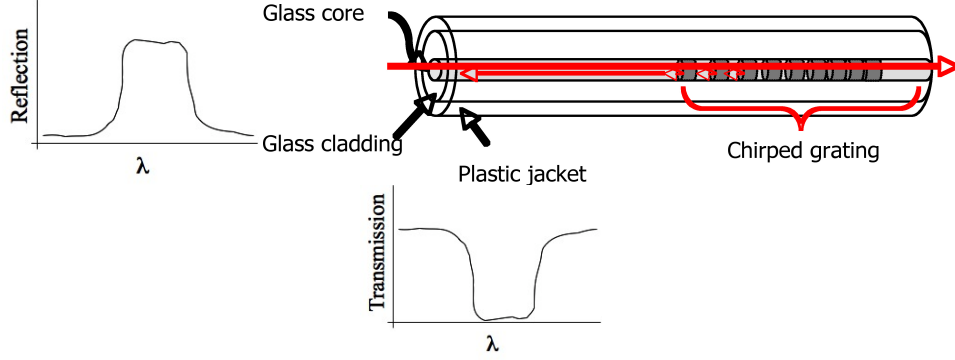


Figure 6. Chirped fiber-optic Bragg grating reflects a finite narrow band of light, while allowing out-of-band light to pass through. The grating bandwidth (and therefore the amount of reflected light) is proportional to the physical length.

Using the Bragg equation
$$\lambda_B = 2n_{eff}\Lambda \quad (1)$$

where n_{eff} is the effective refractive index of the grating and Λ is the period of the grating. The approximate bandwidth of a chirped grating can be given as

$$grating\ bandwidth = \Delta\lambda = |\lambda_{x_{max}} - \lambda_{x_0}| = 2n_{eff}|\Lambda_{x_{max}} - \Lambda_{x_0}| \quad (2)$$

where the x_{max} and x_0 subscripts represent variables taken at the physical ends of the grating.

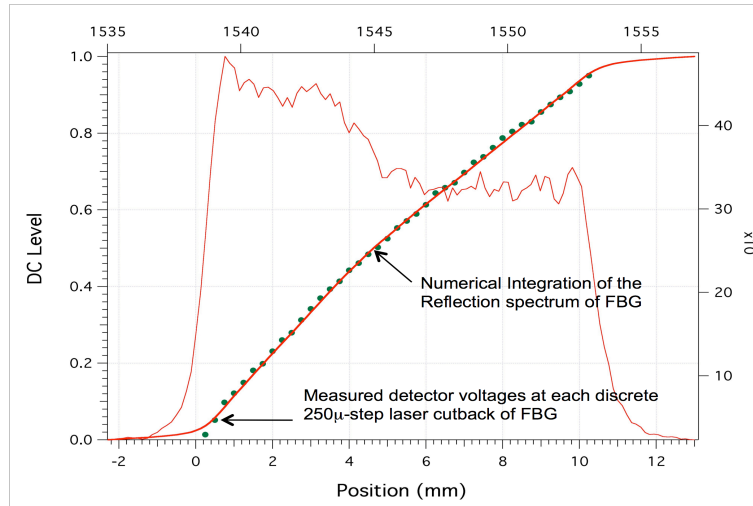


Figure 7. Typical CFBG reflectivity vs. physical length with integral of the entire reflected bandwidth compared to the return intensity after each successive cut.

There is good agreement between detector signal and the numerical integration of the reflection bandwidth. It follows from equation 2 that the integral is also proportional to the *physical length* of the grating. A simple test was done to demonstrate this principle. A CFBG was set on a test stand while connected to instrumentation to measure reflectivity. Laser-trimming the grating shortened the grating in 250 μm increments. The detector signal was recorded after each of 40 laser-cuts until there was no grating left. As seen in figure 7, the detector signal and the numerical integration of the CFBG overlapped with good agreement (except for the very ends of the grating). This test allowed us to measure the physical position vs. wavelength of the grating. It is a destructive test however, leaving no grating for use in subsequent detonation velocity tests. In order to make effective use of a CFBG as an internal detonation velocity sensor, a method to non-destructively measure the *position vs. wavelength* of the CFBG is needed.

Figure 8 shows simple non-destructive measurement of physical position vs. wavelength using a hot-tip micro-probe^[3]. The heated probe tip is scanned along the length of a CFBG. At selected increments, the probe is stopped while observing the CFBG spectrum with a spectrometer. This method, improved by Garrett Cole, can be used to determine the length and location of the CFBG to about 250- μm resolution^[4]. The hot-tip probe method creates local heating and causes a local red shift of the reflected light at the exact position where the heated tip touches the grating. This local heating appears as a dimple in the CFBG spectrum. Using horizontal translation stage, it was relatively easy to create an accurate map of wavelength vs. physical position.

The hot-tip probe method not only revealed the physical position of FWHM points, but also located the -50 dBm points of the CFBG spectrum, thus giving the physical length of the grating.

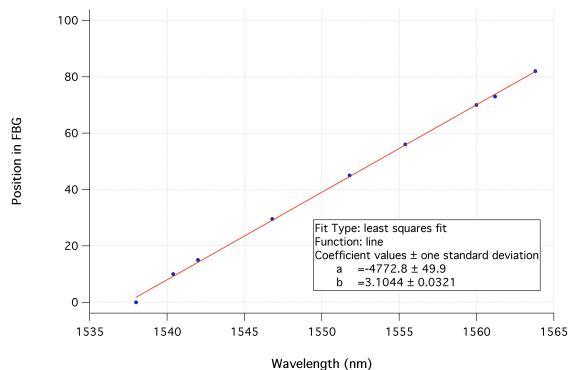
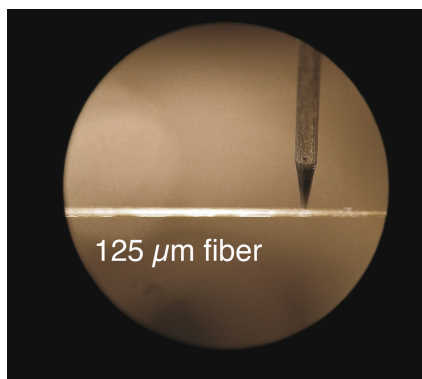


Figure 8. A tungsten probe, heated to 70°C is used to non-destructively measure the location and physical length of a fiber-optic Bragg grating. A high-resolution translation stage was used to precisely position the hot-tip along the length of the fiber. The chirp rate was measured at 3.1 ± 0.03 mm/nm.

Internal detonation velocity measurement of PBX 9502

To test a prototype embedded CFBG detonation velocity sensor, an experiment was designed to measure the internal detonation velocity of a well-characterized explosive (PBX-9502). A CFBG was embedded inside a 4-inch long, 1-inch diameter column PBX-9502. The column was a stack of four 1-inch pellets of PBX-9502. A commercial RP-1 detonator driving a PBX-9407 booster initiated the column. As a timing reference, piezoelectric timing pins were placed along the 4-inch long column of PBX-9502 at 1-inch intervals (see figure 9). Instrumentation consisted of two oscilloscopes to record the pin timing marks, the fireset current viewing resistor (CVR) and the photodiode signal from the CFBG reflection. The CFBG was placed into a 1.6 mm outside diameter Teflon tube with a 175 μ m inside diameter hole. The fiber/tube assembly was pushed through a 1.6 mm hole in the center of the PBX-9502 pellets.

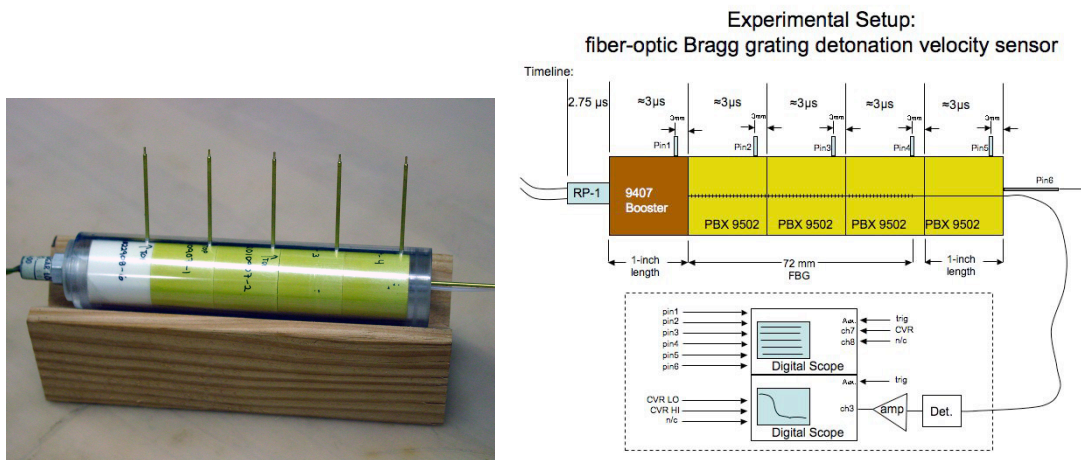


Figure 9. Experimental setup where a CFBG is embedded in a 4-inch column of PBX-9502. The detonation was initiated with a commercial RP-1 detonator followed by a 1 inch PBX-9407 booster. Five piezo timing pins were placed at 1-inch intervals along the length of the PBX-9502 column (right).

The CFBG is illuminated by a broadband ASE source. Light that matches the sensor CFBG's reflection bandwidth is returned. The rest of the ASE light outside the sensor bandwidth passes through the sensor CFBG and is dissipated in the explosive. The return signal is delivered by optical fiber to a photodiode, which produces a voltage proportional to the integral of the reflection bandwidth of the embedded CFBG and the ASE source illumination bandwidth.

The embedded CFGB sensor is destroyed as the detonation wave progresses through the explosive column, thus narrowing the reflection bandwidth of the grating. The photodiode signal is recorded on an oscilloscope during the detonation.

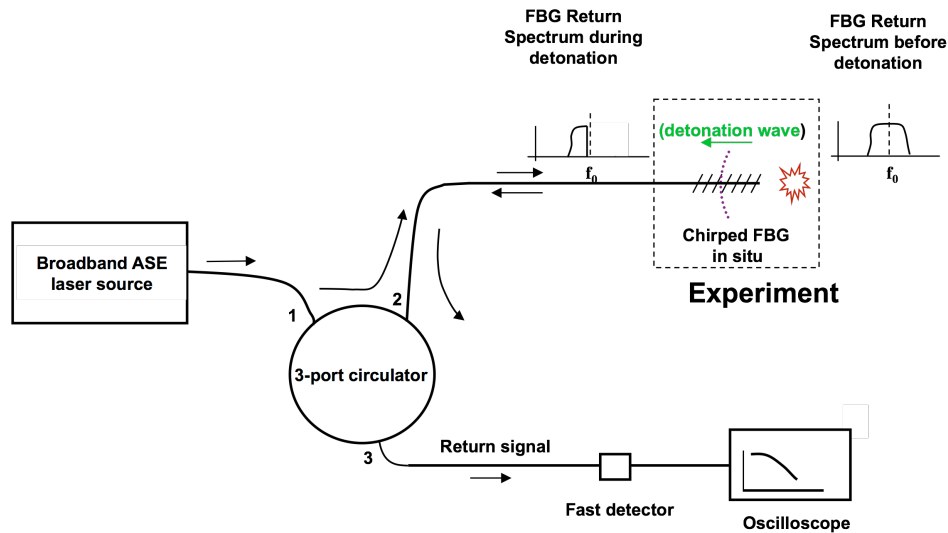


Figure 10. System block diagram of in-situ CFGB detonation velocity sensor.

Analysis of PBX 9502 results

The explosive assembly was test-fired in a 1 kilogram containment tank at LLNL's High Explosives Application Facility (HEAF). Timing pin data and embedded CFGB data were recorded on two separate oscilloscopes, which were triggered from a common trigger source. Figure 11 shows the raw CFGB data is plotted with pin timing marks vs. time. The CFGB sensor data was expected to "bulge" out due to the shape of the integral of the reflection bandwidth (figure 7).

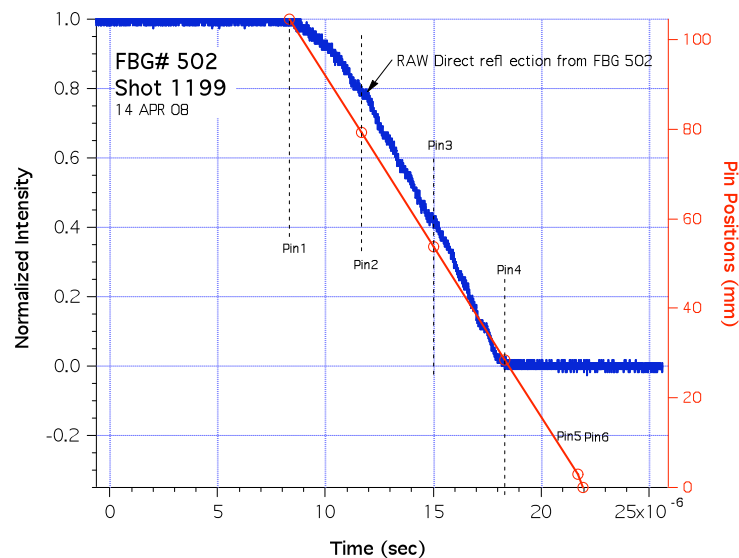


Figure 11. Raw data from test-firing PBX-9502. Raw pin data PBX-9502 average velocity is 7.65 mm/ μ sec. Raw CFGB sensor data had good signal-to-noise ratio compared to an earlier test done in 2007.

Using the integral as a starting point, and assuming an expected detonation velocity of 7.7 mm/ μ sec, a numerical simulation of intensity vs. time was performed (see figure 12). There is very good agreement

between the simulation and the raw sensor data. The experimental data diverges from the simulated data at the ends of the grating where one would expect lower sensitivity to changes in the grating length due to the curvature of the integral in that region.

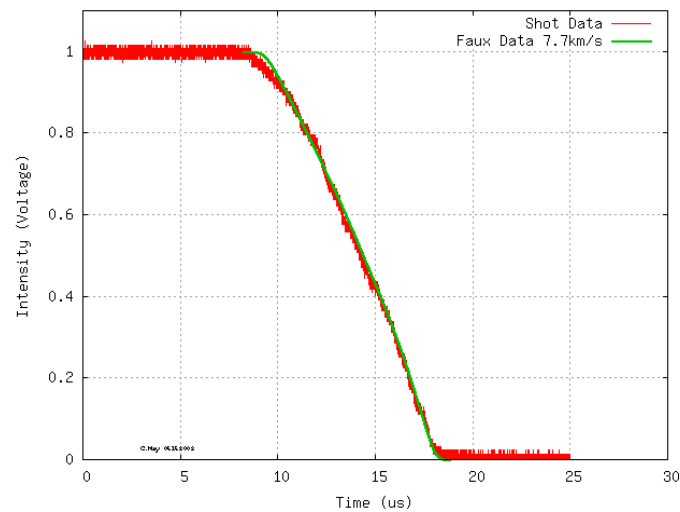


Figure 12. Raw data shows good correlation to numerical simulation of a constant velocity detonation.

The detector sees the return signal coming directly from the CFBG embedded in the HE sample (see the diagram in figure 10). Using the mapping of grating bandwidth vs. reflectivity (figure 7) and wavelength vs. position (figure 8), it is possible to map the position of the detonation wave vs. time, thus giving a continuous time history of the position of a detonation velocity wave inside the high explosive (figure 13).

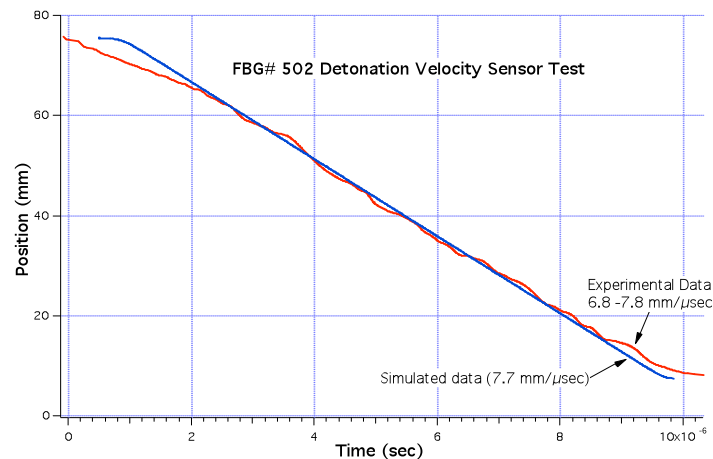


Figure 13. Final data analysis of embedded CFBG #502 velocity sensor. Experimental results agree with numerical simulation in the center portion of the grating.

Surface detonation velocity measurement of C-3 Detasheet

C-3 Detasheet is a plastic explosive available commercially. As shown in figure 14, a 1-inch x 1/2-inch x 1/8-inch piece of Detasheet was placed on an assembly, which also held a commercially available RP-2 detonator. The detonator is used to initiate the Detasheet. A 20 mm long CFBG was sandwiched between a steel plate and the Detasheet explosive. The detonator was connected to the fireset electronics and the fiber was connected to the CFBG receiver system. Figure 10 shows the CFBG receiver system. This time

Two Piezo timing pins were placed along the axis of detonation 20 mm apart. The pins report the arrival time of a traveling detonation wave by producing a voltage spike when shocked. By measuring the time delay between two pins, it is possible to calculate the average velocity of a detonation wave. The pin signals provide a timing reference for the experiment. This test was done to see if it is possible to track a detonation wave as it emerges from the side of the explosive at the interface between the explosive and metal, in this case, steel. The assembly was detonated, giving the results shown in figure 15. As the detonation wave traverses the explosive; the CFBG, which is embedded between the explosive and a steel plate, becomes shorter thus reducing the amount of reflected light returning to the detector. Knowing the transfer function of CFBG length vs. reflection, it's possible to calculate the rate at which the grating is being destroyed, which is the same as the detonation velocity of the explosive. The advantage of this embedded CFBG is that it can continuously track the detonation velocity inside the explosive.

Analysis of C-3 Detasheet results

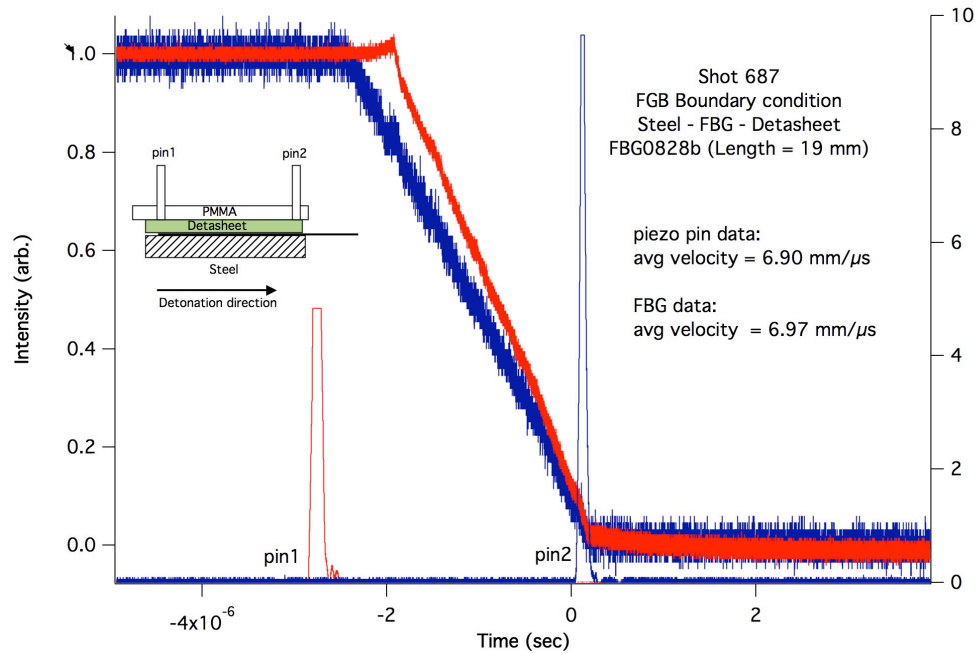


Figure 15. Raw signals captured from CFBG during detonation for the Detasheet. The timing pins placed 20 mm apart give a good indication of the average velocity of the detonation. The red and blue signal traces are from two detectors observing the same CFBG return signal as it is consumed by the detonation. It is at this point it is still not known why the signals look so different.

Using pins, an average detonation velocity was calculated to be 6.90 mm/μs (or 6.90 km/sec). Using the CFBG scope trace, the average velocity was calculated to be 6.97 mm/μs; about a 1% difference. The detonation velocity measured in-situ (inside the explosive) was 6.87 mm/μs in the center portion of the grating. The calculated position vs. time plot, shown in Figure 16, has good agreement with the simulation also shown on the same plot.

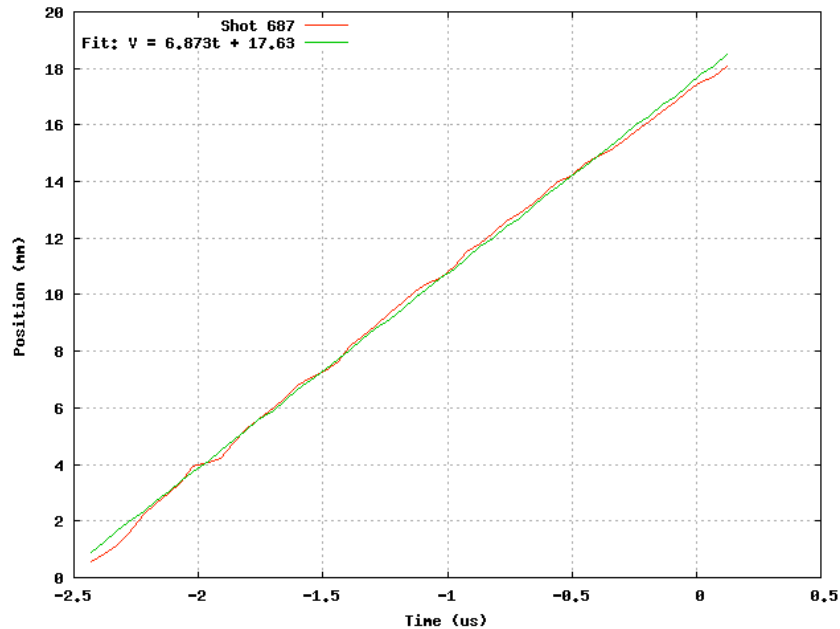


Figure 16. Plot of the calculated in-situ detonation velocity of C-3 Detasheet and the numerical simulation have good agreement. The CFBG detonation velocity sensor measured the velocity in the boundary between the explosive and a steel plate.

Future sensor applications for CFBG detonation velocity sensors

Improvements include establishing techniques using composite (chirped and non-chirped) FBG sensors that have well-defined edges would allow more accurate measurements of the physical length of the sensor. Improvements in the mapping wavelength vs. position could help resolve the uncertainty of detonation velocity at the ends of the grating. For example, a LUNA[®] optical backscatter reflectometer (OBR) has an order of magnitude higher resolution and a two orders of magnitude greater number of data points than the hot-tip probe. These velocity calculations were done assuming that the relationship between wavelength and physical position is a linear function, whereas this function may not be linear near the ends of the grating. Using a high-resolution OBR to more precisely map this wavelength vs. position relationship looks promising.

CFBGs can be placed not only *inside* explosives, but also along boundaries between explosives and metals or other materials. Since embedded CFBG detonation velocity sensors measure the rate of the destruction of the CFBG inside/alongside detonating explosives and shocked materials, these sensors potentially can measure the speed of propagating detonation waves that are not on the axis of the optical fiber.

Additional improvements include developing techniques for drilling extremely small diameter holes in high explosives that would allow the insertion of CFBG sensors into the bulk high explosive. Based on the embedded fiber-optic sensor work done by Dave Hare^[5] et al, we believe that a 125 μm diameter CFBG sensor will cause minimal perturbation to the detonation wave being measured. CFBG sensors can then be placed *inside* high explosives and propellants to measure the detonation velocity and physical parameters associated with very high-speed events.

Conclusions

Fiber-optic Bragg gratings are attractive candidates for real-time monitoring of structures that are exposed to the elements such as bridges and buildings. The glass fiber-optics are resistant to corrosion, are non-magnetic, require little space and require little maintenance once securely installed in the structure. This offers an advantage over conventional electrical sensors.

As a detonation velocity diagnostic, CFBGs offer similar advantages plus the unique capability to be embedded in energetic materials without being so large as to perturb the phenomena one is trying to observe. The results displayed in figures convincingly show that a strong, continuous-in-time signal can be obtained from a CFBG that is closely related to the detonation velocity. Although there are grating end-effects that we don't yet fully understand, our analysis obtains the correct detonation velocity in the central (highest fidelity) portion of the grating.

Acknowledgements

The authors would like to acknowledge the following individuals who helped with some of the experiments described in this paper; Mark Fowler and Steven Mudge, who made all the test hardware and Dan Philips who helped configure the controls and timing electronics for the LLNL experiments.

LLNL-CONF-426425

This work was performed under the auspices of the U.S.
Department of Energy by the Lawrence Livermore National
Laboratory under contract No. DE-AC52-07NA27344

References

References

- [1] T. Clark, E. Udd and J. A. Eck, "Demodulation of Bragg Grating Sensors", Proceedings of SPIE, Vol. 2072, p. 274, 1993.
- [2] E. Udd and T. Clark, "Fiber Optic Grating Sensor Systems for Sensing Environmental Effects", US Patent 5,380,995, Jan. 10, 1995.
- [3] E. Udd and T. Clark, "Sensor Systems Employing Optical Fiber Gratings", US Patent 5,397,891, Mar. 14, 1995.
- [4] E. Udd, K. Corona, K. T. Slattery and D. J. Dorr, "Tension and Compression Measurements in Composite Utility Poles Using Fiber Optic Grating Sensors", Proceedings of SPIE, Vol. 2574, p. 14, 1995.
- [5] E. Udd, K. Corona, K. T. Slattery and D. J. Dorr, "Fiber Grating System Used to Measure Strain in a 22-Foot Composite Utility Pole", Proceedings of SPIE, Vol. 2721, 1996.
- [6] E. Udd, K. Corona-Bittick, J. Dorr, K.T. Slattery, "Low-cost fiber grating sensor demodulator using a temperature-compensated fiber grating spectral filter", Proc. SPIE Vol. 3180, p. 63, 1997.
- [7] E. Udd, K. Corona-Bittick, K. T. Slattery, D. J. Dorr, C. R. Crowe, T. L. Vandiver and R. N. Evans, "Fiber Grating Systems Used to Measure Strain in Cylindrical Structures, Optical Engineering, Vol. 36, p. 1893, 1997.
- [8] J.M. Seim, W.L. Schulz, E. Udd, K. Corona-Bittick, J. Dorr, K.T. Slattery, "Low-Cost High-Speed Fiber Optic Grating Demodulation System for Monitoring Composite Structures", SPIE Proceedings, Vol. 3326, p. 390, 1998.
- [9] J. Seim, W.L. Schulz, E. Udd, M. Morrell, "Higher Speed Demodulation of Fiber Grating Sensors", SPIE Proceedings, Vol. 3670, p. 8, 1999.
- [10] J.M. Seim, W.L. Schulz, E. Udd, H.M. Laylor, S.M. Soltesz, R. Edgar, "Development and Deployment of Fiber Optic Highway and Bridge Monitoring Sensor Systems", SPIE Proceedings, Vol. 3995, p. 479, 2000.
- [11] W. Schulz, J. Conte, E. Udd, J. Seim, "Static and Dynamic Testing of Bridges and Highways using Long-Gage Fiber Bragg Grating Based Strain Sensors", SPIE Proceedings, Vol. 4202, p. 79, 2000.
- [12] E. Udd, J. Seim, W. Schulz, R. McMahon, "Monitoring Trucks, Cars and Joggers on the Horsetail Falls Bridge Using Fiber Optic Grating Strain Sensors", SPIE Proceedings, Vol. 4185, p. 872, 2000.

LLNL-CONF-426425

- [13] W.L. Schulz, J.P. Conte, E. Udd, J.M. Seim, "Seismic Damage Identification using Long Gage Fiber Bragg Grating Sensors", Second Workshop on Advanced Technologies in Urban Earthquake Disaster Mitigation, Kyoto Japan. July 2000.
- [14] W.L. Schulz, J.P. Conte, E. Udd, "Long Gage Fiber Optic Bragg Grating Strain Sensors to Monitor Civil Structures", Proceedings of SPIE, Vol. 4330, p. 56, 2001.
- [15] E. Udd, M. Kunzler, H.M. Laylor, W. Schulz, S. Kreger, J. Corones, R. McMahon, S. Soltesz, R. Edgar, "Fiber Grating Systems for Traffic Monitoring", Proceedings of SPIE, Vol. 4337, p. 510, 2001.
- [16] I. Perez, H.L. Cui, E. Udd, "Acoustic Emission Detection using Fiber Bragg Gratings", Proceedings of SPIE, Vol. 4328, p. 209, 2001.
- [17] W. L. Schulz, J. P. Conte, E. Udd and M. Kunzler, "Structural Damage Assessment Via Model Property Identification Using Macro-Strain Measurements with Fiber Bragg Gratings as an Alternative to Accelerometers", Proceedings of OFS-15, Portland, Oregon, IEEE, p. 67, 2002
- [18] M. Kunzler, E. Udd, T. Taylor, and W. Kunzler, "Traffic Monitoring Using Fiber Optic Grating Sensors on the I-84 Freeway & Future Uses in WIM", Proceedings of SPIE, Vol. 5278, p. 122, 2003.
- [19] S. G. Calvert, J. P. Conte, B. Moaveni, W. L. Schulz and R. de Callalfon, "Real Time Damage Assessment Using Fiber Optic Grating Sensors", Proceeding of SPIE, Vol. 5278, p. 110, 2003.
- [20] M. J. Bartow, S. G. Calvert, and P. V. Bayly, "Fiber Bragg Grating Sensors for Dynamic Machining Applications", Proceedings of SPIE, Vol. 5278, p. 21, 2003.
- [21] E. Udd, S. Calvert, and M. Kunzler, "Usage of Fiber Grating Sensors to Perform Critical Measurements of Civil Infrastructure", Proceedings of OFS-16, Nara, Japan, p. 496, 2003.
- [22] S. Calvert, "High-Speed Dual-Axis Strain Using a Single Fiber Bragg Grating", Proceedings of SPIE, Vol. 5384, p. 229, 2004.
- [23] S. Calvert and J. Mooney, "Bridge Structural Health Monitoring System Using Fiber Grating Sensors: Development and Preparation for a Permanent Installation", Proceedings of SPIE, Vol. 5391, p. 61, 2004.
- [24] J. J. Benterou, E. Udd, P. Wilkins, F. Roeske, E. Roos, D. Jackson "In-situ continuous detonation velocity measurements using fiber-optic Bragg grating sensors", *Proceedings: 34th International Pyrotechnics Seminar V1*, 309-322, Beaune, France (2007).
- [25] E. Udd and J. J. Benterou, "Damage detection system with sub-microsecond resolution", Proceedings of SPIE, Vol. 6933, 2008.
- [26] J. J. Benterou, C. V. Bennett, G. Cole, D. E. Hare, C. May, E. Udd, S. J. Mihailov and P. Lu, "Embedded fiber-optic Bragg grating (FBG) detonation velocity sensor", Proceedings of SPIE, Vol. 7316, 2009.